

# Colchicine prevents disease progression in viral myocarditis via modulating the NLRP3 inflammasome in the cardiosplenic axis

Kathleen Pappritz<sup>1,2,3</sup>, Jie Lin<sup>2</sup>, Muhammad El-Shafeey<sup>1,2,3,4,5</sup>, Henry Fechner<sup>6</sup>, Uwe Kühl<sup>7</sup>, Alessio Alogna<sup>7</sup>, Frank Spillmann<sup>7</sup>, Ahmed Elsanhoury<sup>1,2,3</sup>, Rainer Schulz<sup>4</sup>, Carsten Tschöpe<sup>1,2,3,7</sup> and Sophie Van Linthout<sup>1,2,3\*</sup>

<sup>1</sup>BIH Center for Regenerative Therapies (BCRT), Berlin Institute of Health at Charité, Universitätsmedizin Berlin, Berlin, Germany; <sup>2</sup>Berlin-Brandenburg Center for Regenerative Therapies, Charité-Universitätsmedizin Berlin, Campus Virchow Klinikum (CVK), Berlin, Germany; <sup>3</sup>German Center for Cardiovascular Research (DZHK), Partner site Berlin, Berlin, Germany; <sup>4</sup>Physiologisches Institut, Fachbereich Medizin der Justus-Liebig-Universität, Giessen, Germany; <sup>5</sup>Medical Biotechnology Research Department, Genetic Engineering and Biotechnology Research Institute (GEBRI), City of Scientific Research and Technological Applications, Alexandria, Egypt; <sup>6</sup>Department of Applied Biochemistry, Institute for Biotechnology, Technische Universität Berlin, Berlin, Germany; and <sup>7</sup>Department of Cardiology, Charité – Universitätsmedizin Berlin, CVK, Berlin, Germany

## Abstract

**Aim** The acute phase of a coxsackievirus 3 (CVB3)-induced myocarditis involves direct toxic cardiac effects and the systemic activation of the immune system, including the cardiosplenic axis. Consequently, the nucleotide-binding oligomerization domain-like receptor pyrin domain-containing-3 (NLRP3) inflammasome pathway is activated, which plays a role in disease pathogenesis and progression. The anti-inflammatory drug colchicine exerts its effects, in part, via reducing NLRP3 activity, and has been shown to improve several cardiac diseases, including acute coronary syndrome and pericarditis. The aim of the present study was to evaluate the potential of colchicine to improve experimental CVB3-induced myocarditis.

**Methods and results** C57BL6/j mice were intraperitoneally injected with  $1 \times 10^5$  plaque forming units of CVB3. After 24 h, mice were treated with colchicine (5  $\mu\text{mol/kg}$  body weight) or phosphate-buffered saline (PBS) via oral gavage (p.o.). Seven days post infection, cardiac function was haemodynamically characterized via conductance catheter measurements. Blood, the left ventricle (LV) and spleen were harvested for subsequent analyses. *In vitro* experiments on LV-derived fibroblasts (FB) and HL-1 cells were performed to further evaluate the anti-(fibro)inflammatory and anti-apoptotic effects of colchicine via gene expression analysis, Sirius Red assay, and flow cytometry. CVB3 + colchicine mice displayed improved LV function compared with CVB3 + PBS mice, paralleled by a 4.7-fold ( $P < 0.01$ ) and 1.7-fold ( $P < 0.001$ ) reduction in LV CVB3 gene expression and cardiac troponin-I levels in the serum, respectively. Evaluation of components of the NLRP3 inflammasome revealed an increased percentage of apoptosis-associated speck-like protein containing a CARD domain (ASC)-expressing, caspase-1-expressing, and interleukin-1 $\beta$ -expressing cells in the myocardium and in the spleen of CVB3 + PBS vs. control mice, which was reduced in CVB3 + colchicine compared with CVB3 + PBS mice. This was accompanied by 1.4-fold ( $P < 0.0001$ ), 1.7-fold ( $P < 0.0001$ ), and 1.7-fold ( $P < 0.0001$ ) lower numbers of cardiac dendritic cells, natural killer cells, and macrophages, respectively, in CVB3 + colchicine compared with CVB3 + PBS mice. A 1.9-fold ( $P < 0.05$ ) and 4.6-fold ( $P < 0.001$ ) reduced cardiac gene expression of the fibrotic markers, Col1a1 and lysyl oxidase, respectively, was detected in CVB3 + colchicine mice compared with CVB3 + PBS animals, and reflected by a 2.2-fold ( $P < 0.05$ ) decreased Collagen I/III protein ratio. Colchicine further reduced Col3a1 mRNA and collagen protein expression in CVB3-infected FB and lowered apoptosis and viral progeny release in CVB3-infected HL-1 cells. In both CVB3 FB and HL-1 cells, colchicine down-regulated the NLRP3 inflammasome-related components ASC, caspase-1, and IL-1 $\beta$ .

**Conclusions** Colchicine improves LV function in CVB3-induced myocarditis, involving a decrease in cardiac and splenic NLRP3 inflammasome activity, without exacerbation of CVB3 load.

**Keywords** Coxsackievirus B3; Myocarditis; Colchicine; Cardiosplenic axis; Inflammation

Received: 27 May 2021; Revised: 17 December 2021; Accepted: 4 February 2022

\*Correspondence to: Sophie Van Linthout, BIH Center for Regenerative Therapies (BCRT), Berlin Institute of Health at Charité, Universitätsmedizin Berlin, Charitéplatz 1, 10117 Berlin, Germany. Email: [sophie.van-linthout@charite.de](mailto:sophie.van-linthout@charite.de)  
Carsten Tschöpe and Sophie Van Linthout contributed equally.

## Introduction

Myocarditis is a cardiac disorder, which is characterized by prominent immune cell infiltration in the heart, predominantly due to viral infection. Particularly infections with the enterovirus coxsackievirus B3 (CVB3) are known to cause acute viral myocarditis in young patients.<sup>1–3</sup> In the acute phase of myocarditis, viral entry is not always limited to the heart but may involve other organs, including lymphoid organs such as the spleen.<sup>4</sup> Homing of potentially infected immune cells<sup>4</sup> from the spleen towards the heart takes place and leads to cardiac fibrosis.<sup>5</sup> This cardiosplenic axis must be balanced such that immune-mediated virus-clearing mechanisms are effective without causing aberrant cardiac inflammation, which can trigger myocardial destruction and remodelling that culminates in cardiac dysfunction.<sup>3</sup>

The control of inflammasomes belongs to a critical early response of the host that enables detection of pathogens and endogenous stress signals, initiates production of pro-inflammatory cytokines, and induces recruitment of effector cells to the site of infection. The inflammasome complex is made up of intracellular multiprotein oligomers, which includes a sensor protein such as the nucleotide-binding oligomerization domain (NOD)-like receptor proteins, an adapter protein called apoptosis-associated speck-like protein containing a CARD domain (ASC), and the cysteine protease caspase-1. Triggered by endogenous and exogenous molecules, assembly of the complex leads to autocatalysis and activation of caspase-1, which converts pro-IL-1 $\beta$  into the mature form IL-1 $\beta$ ,<sup>6</sup> which subsequently activates the inflammatory arm of the immune response to infection.

The NOD-like receptor pyrin domain-containing-3 (NLRP3) inflammasome is the most thoroughly described inflammasome complex to date.<sup>6</sup> Its relevance in myocarditis follows from findings of Toldo *et al.*<sup>7</sup> who demonstrated increased formation of the NLRP3 inflammasome in endomyocardial biopsies of myocarditis patients, whereby the severity of heart failure correlated with the intensity of NLRP3 inflammasome formation. In agreement with these findings, we have shown that CVB3 infection up-regulates myocardial NLRP3 expression in experimental and human myocarditis<sup>8,9</sup> and that cardiac NLRP3 expression decreases in CVB3-positive patients who clear the virus over time. Moreover, knockdown of NOD2<sup>9</sup> or treatment with mesenchymal stromal cells<sup>8</sup> protected mice against myocarditis through down-regulation of NLRP3 expression, which was further associated with less migration of immune cells from the spleen towards the heart. Therefore, reduction of NLRP3 inflammasome activity seems to be a potential therapeutic target to control and modify the cardiosplenic axis in acute myocarditis. The

anti-inflammatory drug colchicine inhibits NLRP3 activity<sup>10</sup> as part of its well-known microtubule-disassembling properties.<sup>11</sup> Furthermore, anti-fibrotic effects of colchicine have also been reported.<sup>12</sup> Its recommendation for use as a first-line therapy for treatment of acute pericarditis, which, similar to myocarditis is often of viral origin,<sup>13,14</sup> further supports the hypothesis that colchicine could be also useful in the treatment of myocarditis.

This proof-of-concept study was conducted with the aim of investigating the impact of colchicine in experimental CVB3-induced myocarditis and of gaining insights into the underlying mechanisms of how colchicine functions. Given the fact that colchicine is inexpensive and its use worldwide is established, colchicine could be an ideal candidate for the treatment of potentially all forms of virus-induced myocarditis, including SARS-CoV2-related myocarditis syndromes.<sup>3</sup>

## Methods

### Experimental coxsackievirus B3-induced acute myocarditis

To induce viral myocarditis, 6 week old male C57BL6/j mice were purchased from Charles River (Sulzfeld, Germany) and housed in the animal facilities of the *Charité - Universitätsmedizin Berlin* under standard housing conditions (12 h light/dark cycle, 50–70% humidity, 19–21°C). Animals were housed with 4–5 mice per cage with unlimited access to food and water. At the age of 8 weeks, mice were randomly divided into four groups. Two of these groups (CVB3 and CVB3 + colchicine group) were intraperitoneally (i.p.) injected at the age of 8 weeks with 200  $\mu$ L phosphate-buffered saline (PBS) (Life Technologies, Carlsbad, CA, USA) containing  $1 \times 10^5$  plaque forming units (p.f.u) of CVB3 (Nancy strain). Control mice (control and colchicine group) received the same volume (200  $\mu$ L) of PBS (Life Technologies) alone. Twenty-four hours after CVB3 infection, mice were treated either with 5  $\mu$ mol/kg body weight (BW) colchicine (Merck Millipore, Darmstadt, Germany; colchicine group and CVB3 + colchicine group) or PBS (Life Technologies; control and CVB3 group) via oral gavage. Seven days post infection, left ventricular (LV) function was determined via conductance catheter as reported in detail in the following paragraph.<sup>15</sup> Subsequently, mice were euthanized via cervical dislocation, and serum and LV were collected for ELISA, gene expression analysis, caspase 3/7 assay, immunohistochemistry, and plaque assay. The respective *n*-number of each group used for each molecular

investigation is indicated in the respective figure legend. Due to the limited amount of available tissue material, not all investigations could be performed for the whole set of animals. In a second set of experiments ( $n = 8/\text{group}$ , whereby 2 animals per group were pooled for cell isolation) with the same experimental design, mice were euthanized via cervical dislocation without prior haemodynamic measurement. For subsequent flow cytometry, LV and spleen were harvested and stored on ice until further processing. All experiments were performed according to the European legislation for the Care and Use of Laboratory Animals (Directive 2010/63/EU) and approved by the local ethics committee (Landesamt für Gesundheit und Soziales, Berlin, G0310/15).

### Haemodynamic characterization

To determine the effect of colchicine on cardiac function, mice were haemodynamically characterized using conductance catheter. Animals were anaesthetized with a mixture of 1.2 g/kg BW urethane (Sigma-Aldrich Chemie GmbH, Steinheim, Germany) and 0.05 mg/kg BW buprenorphine (Indivior UK limited, Slough, UK) followed by mechanical ventilation. For continuous recording of pressure-volume loops in an open-chest model, a 1.2 F conductance catheter (SciSense, Ontario, Canada) was apically positioned in the LV. In addition to heart rate (bpm), LV ejection fraction (EF; %), cardiac output (CO;  $\mu\text{L}/\text{min}$ ), LV maximal pressure ( $\text{LVP}_{\text{max}}$ ; mmHg), end-systolic pressure ( $P_{\text{es}}$ ; mmHg), end-diastolic pressure ( $P_{\text{ed}}$ ; mmHg), LV contractility ( $dP/dt_{\text{max}}$ ; mmHg/s), LV relaxation ( $dP/dt_{\text{min}}$ ; mmHg/s), and LV relaxation time ( $\text{Tau}$ ; ms) as indices for cardiac function were assessed.<sup>16</sup>

### Serum troponin-I ELISA

As a biochemical marker for myocardial damage, cardiac troponin-I (cTN-I) was measured in the serum of controls and CVB3-infected mice treated with or without colchicine. For this purpose, a commercially available ultra-sensitive mouse cTN-I ELISA (Life Diagnostics, West Chester, PA, USA) was performed according to the manufacturer's protocol.

### Gene expression analysis

According to established protocols, RNA extraction from LV tissue was performed using the TRIzol™ method. In case of the *in vitro* experiments, FB were harvested after 24 h and washed twice with PBS. Afterwards, 1 mL TRIzol™ was added, followed by chloroform extraction and precipitation. Purification of the samples was performed via the NucleoSpin® RNA mini kit (Macherey-Nagel GmbH, Düren, Germany). For sub-

sequent cDNA transcription, 1000 ng of the total RNA and the high-capacity cDNA Reverse Transcription Kit (Applied Biosystems, Darmstadt, Germany) was used. To perform quantitative real-time PCR, a QuantStudio 6 Flex Real-Time PCR System (Thermo Fisher Scientific, Darmstadt, Germany) and the following gene expression assays (all provided by Applied Biosystems, Darmstadt, Germany) were used:  $\alpha$ -smooth muscle actin ( $\alpha$ -SMA; Mm00725412\_s1), B-cell lymphoma 2 (Bcl-2; Mm00477631\_m1), Bcl-2-associated X protein (Bax; Mm00432050\_m1), caspase-3 (Casp3; Mm00438045\_m1), Col1a1 (Mm01302043\_g1), Col3a1 (Mm00802331\_m1), lysyl oxidase (Lox; Mm00495386\_m1), NADPH Oxidase 1 (NOX1; Mm00549170\_m1), NADPH Oxidase 4 (NOX4; Mm00479246\_m1), mitochondrial superoxide dismutase 2 (SOD2; Mm01313000\_m1), and transforming growth factor- $\beta$  (TGF- $\beta$ ; Mm00441724\_m1). Furthermore, CVB3 copy numbers in LV tissue samples were detected via a forward primer (5'-CCCTGAATGCGGCTAATCC-3'), reverse primer (5'-ATTGTCACCATAAGCAGCCA-3'), and FAM-labelled MGB probe (FAM 5'-TGCAGCGGAACCG-3'). For quantification, data were first normalized to the endogenous control, Glyceraldehyde-3-phosphate dehydrogenase (GAPDH; Mm99999915\_g1) and afterwards to the control group, set as 1.

### Plaque assay

To determine viral progeny release of CVB3-infected HL-1 cells and LV viral load, a plaque assay was performed. Supernatant of untreated or colchicine-treated HL-1 cells 24 h post infection and homogenized LV tissue samples of CVB3 + PBS and CVB3 + colchicine mice were analysed, as previously described.<sup>15,17</sup> In detail, HeLa cells were overlaid with 300  $\mu\text{L}$  of the LV lysates and incubated for 30 minutes (min) at 37°C. Afterwards, supernatant was removed and cells were overlaid with 500  $\mu\text{L}$  agar containing Eagle's MEM. After 3 days, the virus titre was determined by plaque counting and depicted as p.f.u./mL or p.f.u./heart weight (mg), respectively.

### Preparation of left ventricle and spleen homogenates

For subsequent investigations on protein level, tissue homogenates of LV and spleen (with  $n = 5\text{--}6/\text{group}$  and organ) were prepared. To this end, the respective tissue was homogenized in 200  $\mu\text{L}$  cell lysis buffer (Thermo Fisher Scientific) using the Precellys homogenizer (Bertin Technologies SAS, Montigny-le-Bretonneux, France). After 20 min incubation on ice, samples were centrifuged at 13 500 rpm and 4°C for 15 min. Afterwards, supernatant was transferred, and protein amount was determined via the Pierce™ BCA Protein Assay Kit (Thermo Fisher Scientific).

### Caspase 3/7 assay of left ventricle tissue homogenates

To determine apoptotic processes in LV tissue, a caspase 3/7 activity assay (Promega, Madison, WI, USA) was performed. In detail, LV homogenates were prepared as described earlier. Afterwards, 100  $\mu$ L of the lysates containing 250  $\mu$ g protein were added to a white-walled 96-well luminometer plate. According to the manufacturer's protocol and as described previously,<sup>17,18</sup> 100  $\mu$ L of the caspase-Glo 3/7 reagent containing caspase 3/7 buffer and the pro-luminescent caspase 3/7 substrate, was added to each sample. After 60 min of incubation at room temperature, the luminescence of each sample was measured in a microplate-reading luminometer (Mithras LB 940, Berthold Technologies GmbH & Co KG, Germany).

### Coxsackievirus B3 infection of HL-1 cardiomyocytes

The subsequently described experiment was performed using the murine cardiomyocyte cell line HL-1. Before cell plating, 6-well plates were coated with 0.02% gelatin (Sigma-Aldrich Chemie GmbH) for 30 min at 37°C. Thereafter, 225 000 HL-1 cells/well were plated in full Claycomb medium (Sigma-Aldrich Chemie GmbH) supplemented with 10% foetal bovine serum (FBS; Biochrom, Berlin, Germany), 1% penicillin/streptomycin (P/S, Life Technologies), 0.1 mmol/L norepinephrine (Sigma-Aldrich Chemie GmbH), and 2 mmol/L L-glutamine (Biochrom) into 6-well plates. Twenty-four hours later, cells were either infected with CVB3 (Nancy Strain) at a multiplication of infection (m.o.i.) of two in serum starvation medium [DMEM 11966 (Gibco, Thermo Fisher Scientific, Darmstadt, Germany)] + 5 mM Glucose (Sigma-Aldrich Chemie GmbH) + 0.01% FBS (Biochrom), or incubated with serum starvation medium only, both for 2 h. One hour post-CVB3-infection or serum starvation, cells were incubated in the presence of 100 ng/mL colchicine (Merck Millipore, Darmstadt, Germany) or PBS (Thermo Fisher Scientific, Darmstadt, Germany). Supernatant and cells were collected 24 h after CVB3 infection for viral progeny release and flow cytometry analyses of apoptotic cells, respectively. Furthermore, expression of NLRP3 inflammasome-related proteins (ASC, caspase-1, and IL-1 $\beta$ ) were analysed after 4 h of stimulation with colchicine using flow cytometry.

### Flow cytometry

To investigate the expression of the NLRP3 inflammasome-related proteins ASC, caspase-1, and IL-1 $\beta$  in the heart and spleen of mice upon CVB3 infection and subsequent treatment with/without colchicine, a second set of *in vivo* experiments was performed as described earlier. In brief, mice were

euthanized under anaesthesia via cervical dislocation without prior haemodynamic measurement. Subsequently, LV and spleen were harvested and stored on ice for cardiac mononuclear cell (MNC) or splenocyte isolation.<sup>19</sup> After cell isolation, expression of ASC, caspase-1, and IL-1 $\beta$  in total and specifically on dendritic cells (DC; CD11c<sup>+</sup> cells), natural killer (NK) cells (CD49<sup>+</sup> cells), and macrophages (F4/80<sup>+</sup> cells) was analysed in the heart and the spleen.<sup>8</sup> For this purpose,  $1 \times 10^6$  splenocytes or  $0.9\text{--}1.2 \times 10^6$  cardiac MNCs were fixed and permeabilized in Cytotfix/Cytoperm buffer (BD Biosciences, Heidelberg, Germany). After washing and centrifugation, samples were stained with the respective anti-ASC (BioLegend, Koblenz, Germany), anti-caspase-1 (p10; Bioss Antibodies, Woburn, MA, USA), anti-CD11c (Biolegend, San Diego, CA, USA), anti-CD49 (Biolegend), anti-F4/80 (Biolegend), and anti-IL-1 $\beta$  (BioLegend) antibodies.

For the assessment of early apoptosis of HL-1 cells following CVB3 infection, Annexin V<sup>+</sup>/7AAD<sup>-</sup> flow cytometry was performed as described previously.<sup>17</sup> Twenty-four hours post-CVB3 infection or serum starvation, cells were harvested and washed twice with cold cell staining buffer (Biolegend, Koblenz, Germany) for subsequent Annexin V<sup>+</sup> and 7AAD<sup>-</sup> staining. After the last wash step, cells were re-suspended in 100  $\mu$ L Annexin-binding buffer (BioLegend). Next, 5  $\mu$ L anti-Annexin V and 5  $\mu$ L of anti-7AAD were added and incubated at room temperature for 15 min in the dark. After incubation, 400  $\mu$ L Annexin-binding buffer was added for measurement.

In addition to the measurement of early apoptosis, ASC, caspase-1, and IL-1 $\beta$  expression were also assessed in HL-1 cells or FB. For this, cells were harvested after 4 h stimulation time and subsequently fixed and permeabilized in Cytotfix/Cytoperm buffer (BD Biosciences). After washing procedure, cells were stained with anti-ASC (BioLegend), anti-caspase-1 (p10; Bioss Antibodies), and anti-IL-1 $\beta$  (BioLegend) antibodies.

After the respective stainings, measurements were performed on a MACSQuant Analyzer (Miltenyi Biotec, Bergisch Gladbach, Germany). Next, data were analysed with the FlowJo software version 8.7 (Tree Star Inc., Ashland, VA, USA) and expressed as percentage (%) of gated cells or as number of events (cell counts).

### IL-1 $\beta$ ELISA

To investigate IL-1 $\beta$  protein on a systemic and organ level, the commercially available IL-1 $\beta$  ELISA (R&D Systems Inc., McKinley Place NE, MN, USA) was performed using LV homogenates, serum, and spleen homogenates. In brief, 50  $\mu$ L of LV or spleen homogenates containing 250  $\mu$ g protein and 50  $\mu$ L undiluted serum were added per well. All further steps were performed according the manufacturer's protocol. Optical density was determined at 540 and 450 nm, whereby readings at 540 nm were subtracted from the readings at 450 nm.

## Immunohistochemistry

First, frozen LV tissue samples were embedded in Tissue-Tek OCT (Sakura, Zoeterwoude, NL) and cut into 5  $\mu\text{m}$  thick sections for subsequent immunohistological investigations. To this end, slides were incubated with the following antibodies: anti-collagen I (dilution 1:350; Chemicon, Merck Millipore, Darmstadt, Germany) and anti-collagen III (dilution 1:200; Calbiochem, Merck Millipore, Darmstadt, Germany) using the EnVision<sup>®</sup> method. After the respective staining, samples were investigated on a Leica DM2000 LED microscope (Leica Microsystems GmbH, Wetzlar, Germany) at 100 $\times$  magnification, followed by digital image analysis via the Leica Application Suite version 4.4 (LAS V4.4). In general, specific epitopes of the stained structure are coloured red and the heart area (HA) was counterstained with Hemalum (blue). To distinguish between different types of fibrosis, LV samples were analysed including vessel and arteries (total LV area) and without vessels and arteries (interstitial fibrosis).

## Coxsackievirus B3 infection of murine primary fibroblasts derived from the left ventricle

To investigate the impact of colchicine on inflammasome activation and the fibrotic response upon CVB3 infection in cardiac fibroblasts, *in vitro* experiments with murine LV-derived fibroblasts (FB) were performed. For this purpose, cells were obtained via outgrowth culture according to our established protocol.<sup>16</sup> At passage 9, cells were seeded either at a cell density of 10 000 cells per well for Sirius red and crystal violet assay or 150 000 cells per well for gene expression analysis and flow cytometry. As seeding media, DMEM high glucose media (Gibco; Thermo Fisher Scientific) supplemented with 20% FBS (Bio&Sell GmbH, Feucht bei Nürnberg, Germany) and 1% P/S (Gibco) was used. Twenty-four hours later, FB were infected at a m.o.i. of 2 in serum starvation medium [DMEM 11966 (Gibco) + 5 mM Glucose (Sigma-Aldrich Chemie GmbH) + 0.01% FBS (Bio&Sell GmbH)] or incubated with pure serum starvation medium. After 1 h incubation, cells were washed twice with PBS (Gibco), followed by treatment with DMEM high glucose (Gibco) containing 10% FBS (Bio&Sell GmbH) and 1% P/S (Gibco) with or without 100 ng/mL colchicine. Depending on the respective experiment, cells were stimulated up to 72 h.

## Sirius red and crystal violet assay

To determine the anti-fibrotic potential of colchicine, a Sirius red and crystal violet assay were performed according to our established protocols.<sup>20,21</sup> In detail, cells were seeded at a cell density of 10 000 cells per well in 96-well plates, infected,

and stimulated as described in the respective paragraph. After 24 or 72 h of stimulation, media was removed and plates were either fixated with cold methanol (Carl Roth, Karlsruhe, Germany) or 4% paraformaldehyde (PFA; SAV Liquid Production GmbH, Flintsbach am Inn, Germany). The methanol-fixated plates were used for subsequent Sirius red staining (Sigma-Aldrich Chemie GmbH) to measure collagen deposition. In parallel, crystal violet staining (Sigma-Aldrich Chemie GmbH) on the PFA-fixated plates was performed to determine the cell number per well. The photometric analyses were performed at 540 or 595 nm using the Spectra Max 340PC microplate reader (Molecular Device GmbH LLC, San Jose, CA, USA). Absorbance values were depicted separately (collagen deposition and cell count) or normalized (collagen content/cell number).

## Statistical analysis

Statistical analysis was performed using Graph Pad Prism 8.0 (GraphPad Software, La Jolla, USA). Data are depicted as scatter plots with bars, showing individual data points and the mean  $\pm$  SEM and were tested for normal distribution using the Shapiro–Wilk test. For normally distributed data, ordinary one-way ANOVA with Sidak's post hoc test was performed. In case data were not normally distributed, Brown–Forsythe and Welch-ANOVA followed by unpaired *t* test with Welch's correction was performed. All *in vitro* experiments were analysed via Brown–Forsythe and Welch-ANOVA followed by unpaired *t* test with Welch's correction. Differences were considered statistically significant at  $P < 0.05$ .

## Results

### Colchicine improves left ventricular function and decreases cardiac troponin-I in experimental Coxsackievirus B3-induced myocarditis

The CVB3-induced myocarditis mice were characterized by impaired global heart function, as indicated by a decline in LV EF and CO (Table 1). In parallel, systolic and diastolic function was reduced as shown by 2.1-fold ( $P < 0.0001$ ) lower  $dP/dt_{\text{max}}$ , 2.4-fold ( $P < 0.0001$ ) lower  $dP/dt_{\text{min}}$ , and 2.3-fold ( $P < 0.01$ ) elevated Tau compared with uninfected control animals. In addition,  $LVP_{\text{max}}$  was 1.4-fold ( $P < 0.01$ ) reduced in control vs. CVB3-infected mice. Related to end-diastolic LV pressure, no differences between control and CVB3 mice were observed. Treatment with colchicine abrogated the adverse effects on LV function in CVB3-infected mice, indicated by improved EF and CO. Furthermore, higher  $dP/dt_{\text{max}}$ ,  $dP/dt_{\text{min}}$  and lower Tau values were observed in CVB3 + colchicine mice vs. CVB3 mice, indicative for an improved systolic and

**Table 1** Colchicine improves left ventricular function and decreases cardiac troponin I levels in experimental Coxsackievirus B3-induced myocarditis

	Control	Colchicine	CVB3	CVB3 + colchicine
Left ventricular function				
HR	510.6 ± 12.19	544.0 ± 8.92	407.3 ± 32.38**	479.2 ± 18.19 <sup>#</sup>
EF	78.20 ± 0.82	78.08 ± 1.27	67.25 ± 2.26****	73.56 ± 1.306 <sup>#</sup>
CO	20 780 ± 1996	26 724 ± 1983	10 099 ± 2395**	17 875 ± 1758 <sup>#</sup>
LVP <sub>max</sub>	102.1 ± 6.81	112.7 ± 4.13	71.10 ± 7.06**	103.3 ± 3.75 <sup>###</sup>
P <sub>es</sub>	94.64 ± 7.49	104.2 ± 4.79	66.01 ± 7.40*	99.37 ± 3.86 <sup>#</sup>
P <sub>ed</sub>	7.47 ± 0.95	10.07 ± 0.77	7.039 ± 0.68	8.90 ± 0.86
dP/dt <sub>max</sub>	8847 ± 560.3	10 186 ± 462.2	4278 ± 759.1****	8344 ± 264.7 <sup>####</sup>
dP/dt <sub>min</sub>	-5631 ± 423.2	-7038 ± 375.9	-2389 ± 440.5****	-5118 ± 302.0 <sup>####</sup>
Tau	12.05 ± 0.67	10.71 ± 0.55	27.23 ± 4.20**	14.04 ± 0.96 <sup>#</sup>
Myocardial damage				
cTN-I	5.78 ± 0.60	6.70 ± 0.57	8.68 ± 0.70*	5.45 ± 0.52 <sup>###</sup>

As indices for global left ventricular (LV) function, heart rate (HR; bpm), cardiac ejection fraction (EF; %) and cardiac output (CO; µL/min) were obtained via conductance catheter measurements. Additionally, LV maximal pressure (LVP<sub>max</sub>; mmHg), end-systolic pressure (P<sub>es</sub>; mmHg), end-diastolic pressure (P<sub>ed</sub>; mmHg), LV contractility (dP/dt<sub>max</sub>; mmHg/s), LV relaxation (dP/dt<sub>min</sub>; mmHg/s) and LV relaxation time (Tau; ms) were analysed. Measurements were performed in control mice or CVB3-infected mice treated with phosphate-buffered saline (PBS) or 5 µmol/kg BW colchicine. As a marker for myocardial damage, cardiac Troponin-I (cTN-I; ng/mL) in the serum was measured via ELISA. Data are presented as mean ± SEM. Statistical analysis was performed by using ordinary one-way ANOVA or Welch-ANOVA.

\**P* < 0.05.

\*\**P* < 0.01.

\*\*\**P* < 0.001.

\*\*\*\**P* < 0.0001 vs. control mice.

<sup>#</sup>*P* < 0.05.

<sup>##</sup>*P* < 0.01.

<sup>###</sup>*P* < 0.001.

<sup>####</sup>*P* < 0.0001 vs. CVB3 mice; with *n* = 11/control + PBS, *n* = 13/control + colchicine, *n* = 11/CVB3 + PBS, and *n* = 16/CVB3 + colchicine.

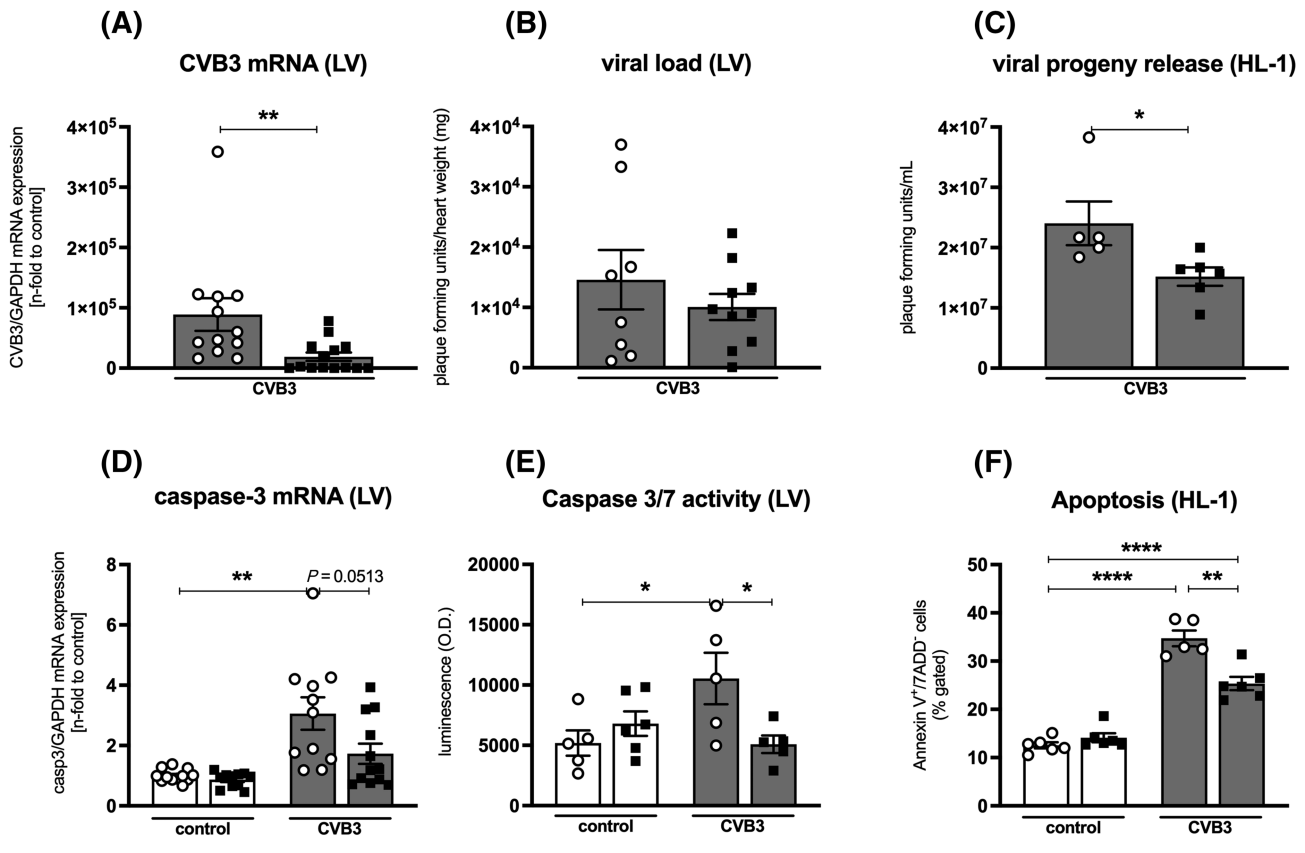
diastolic function, respectively. Administration of colchicine in CVB3 mice led to a 1.5-fold (*P* < 0.001) improvement of LVP<sub>max</sub> compared with PBS treatment. In addition to haemodynamic parameters, cardiac troponin-I (cTN-I), a marker for myocardial damage, was measured in the serum of mice. As shown in *Table 1*, CVB3 mice displayed 1.5-fold (*P* < 0.05) higher cTN-I levels compared with controls. Colchicine was able to diminish myocardial damage, as indicated by the 1.6-fold (*P* < 0.001) reduced cTN-I levels in CVB3 + colchicine mice vs. CVB3 mice.

### Colchicine leads to reduced viral gene expression, apoptosis, and oxidative stress in experimental Coxsackievirus B3-induced myocarditis

The impaired cardiac function in CVB3 mice was associated with LV CVB3 presence, as indicated by LV CVB3 mRNA levels and viral load in CVB3 animals (*Figure 1A + B*). Colchicine treatment in CVB3 animals reduced LV CVB3 mRNA expression by 4.7-fold (*P* < 0.01) (*Figure 1A*), while the LV viral load in CVB3 + colchicine mice only tended to be lower compared with CVB3 + PBS mice (1.5-fold; *P* = 0.4209) (*Figure 1B*). *In vitro*, viral progeny release was less pronounced upon colchicine-treated vs. untreated CVB3-infected HL-1 cells (*Figure 1C*). Because cardiomyocyte apoptosis is known to underlie viral progeny release,<sup>17</sup> we next investigated whether colchicine decreases CVB3-induced apoptosis in the LV and in HL-1 cardiomyocytes (*Figure 1C–F*). As a

marker for *in vivo* cardiac apoptosis,<sup>22,23</sup> LV gene expression of the anti-apoptotic Bcl-2 and pro-apoptotic Bax were analysed and the subsequent ratio calculated (*Figure S1A–C*). In detail, CVB3 mice displayed a 1.7-fold (*P* < 0.01) and 2.2-fold (*P* < 0.001) induced LV Bcl-2 and Bax gene expression compared with controls, which was diminished by the application of colchicine. In accordance with previous own findings,<sup>24</sup> the Bcl-2/Bax ratio did not differ between the groups. In addition, we could confirm our own previous observations,<sup>17,18</sup> reporting increased LV caspase-3 gene expression (*Figure 1D*) and caspase 3/7 activity (*Figure 1E*) upon CVB3 infection. Colchicine treatment abrogated cardiac apoptosis as indicated by a 2.1-fold (*P* < 0.05) decrease in LV caspase 3/7 activity. *In vitro*, colchicine lowered the percentage of CVB3-induced Annexin V<sup>+</sup>/7AAD<sup>-</sup> HL-1 cells by 1.4-fold (*P* < 0.0001), indicative for early apoptotic cells (*Figure 1F*). Finally, knowing that oxidative stress triggers apoptosis in experimental myocarditis,<sup>24,25</sup> LV gene expression of the oxidative stress markers NOX1, NOX4, and of the enzyme SOD2, counteracting oxidative stress, was investigated (*Figure S1D–F*). Compared with controls, CVB3 mice exhibited 24-fold (*P* < 0.0001) and 4.3-fold (*P* < 0.0001) higher LV mRNA levels of NOX1 and NOX4, respectively (*Figure S1D + E*). In contrast, LV SOD2 gene expression was 1.4-fold (*P* < 0.01) reduced in CVB3-infected mice vs. control animals (*Figure S1F*). Treatment with colchicine reduced LV NOX1 and NOX4 mRNA levels, whereas SOD2 gene expression was increased.

**Figure 1** Colchicine leads to reduced viral gene expression, decreased viral progeny release, and less apoptosis in experimental Coxsackievirus B3-induced myocarditis. The impact of colchicine on (A) CVB3 expression and (B) viral load in CVB3-infected mice (grey bars) treated with phosphate-buffered saline (PBS) (o) or 5  $\mu\text{mol/kg}$  BW colchicine (■) was analysed by real-time PCR and plaque assay, respectively. *In vitro*, colchicine reduced CVB3-induced viral progeny release in HL-1 cardiomyocytes (C). Graphs represent viral progeny release in CVB3-infected HL-1 cells (grey bars) treated without (o) or with 100 ng/mL colchicine (■). To determine apoptosis, LV caspase 3 mRNA level (D) and caspase 3/7 activity (E) were assessed by real-time PCR and luminescence measurements, respectively. In parallel, the effect of *in vitro* infection of HL-1 cells and subsequent treatment with colchicine on apoptosis was investigated via flow cytometry. In detail, the percentage of Annexin V + /7AAD- HL-1 cells was determined (F). Data are depicted as scatter plots with bars, showing individual data points and the mean  $\pm$  SEM. Statistical analyses were performed with Mann–Whitney test for LV CVB3 gene expression (\*\* $P < 0.01$ ,  $n = 12/\text{CVB3} + \text{PBS}$  and  $n = 14/\text{CVB3} + \text{colchicine}$ ; A) and with unpaired  $t$  test with Welch's correction for plaque assay data (with  $n = 8/\text{CVB3} + \text{PBS}$  and  $n = 10/\text{CVB3} + \text{colchicine}$ ; B). Data of the HL-1 plaque assay were statistically analysed with Mann–Whitney test (\* $P < 0.05$  with  $n = 5\text{--}6/\text{group}$ ). In graph (D–F), statistical analysis was performed by using ordinary one-way ANOVA or Welch-ANOVA (\* $P < 0.05$ , \*\* $P < 0.01$ , \*\*\* $P < 0.001$ , and \*\*\*\* $P < 0.0001$ ; with  $n = 11\text{--}12/\text{control} + \text{PBS}$ ,  $n = 11\text{--}15/\text{control} + \text{colchicine}$ ,  $n = 11\text{--}12/\text{CVB3} + \text{PBS}$ ,  $n = 12\text{--}13/\text{CVB3} + \text{colchicine}$  for D, and  $n = 5\text{--}6/\text{group}$  for E + F).

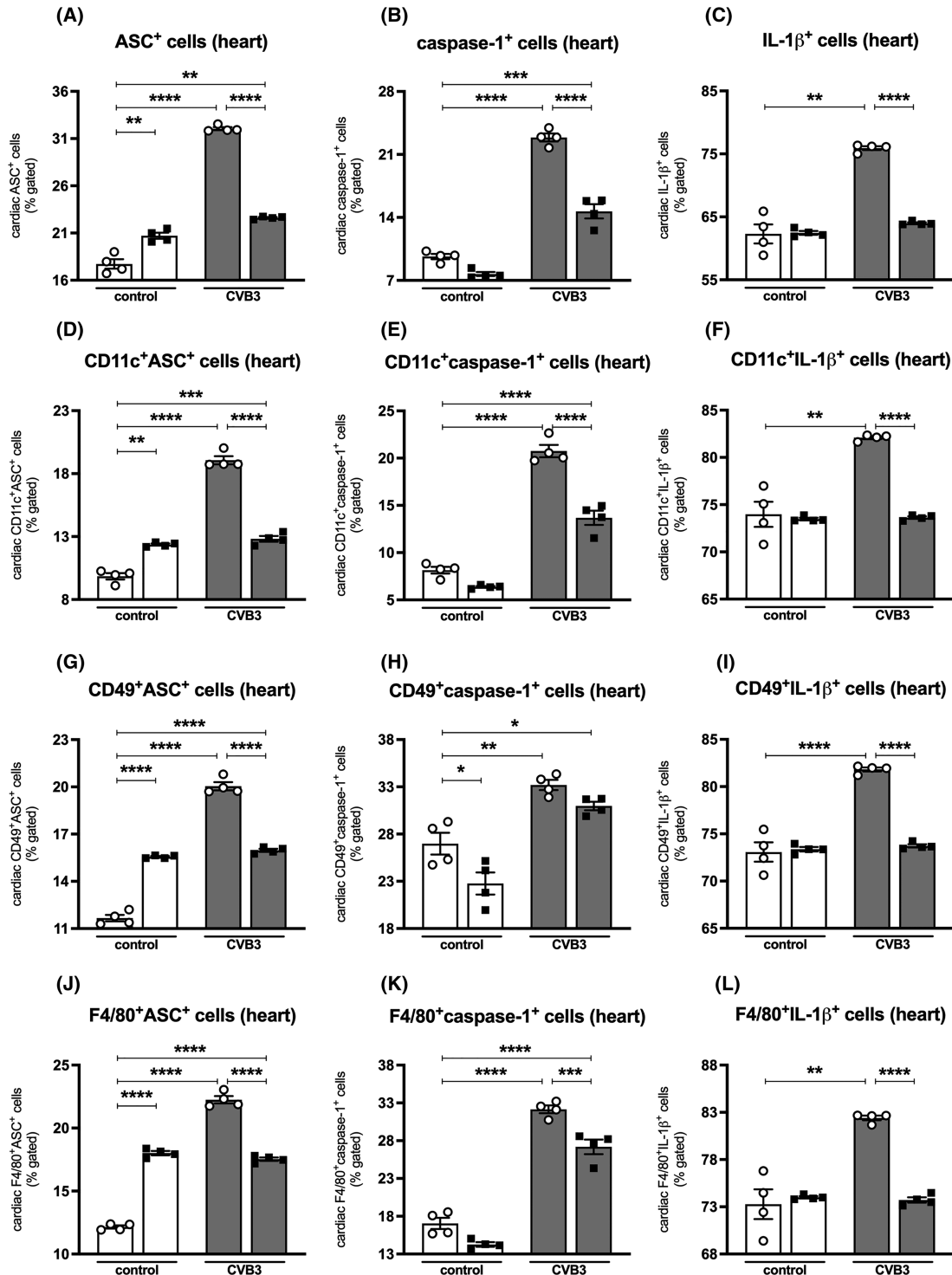


### Colchicine reduces left ventricular NLRP3 inflammasome activity in experimental Coxsackievirus B3-induced myocarditis

Given the relevance of the cardiac NLRP3 inflammasome in CVB3 myocarditis<sup>7–9</sup> and the capacity of colchicine to reduce NLRP3 inflammasome activity,<sup>10</sup> we next investigated the impact of colchicine on NLRP3 inflammasome activity in cardiac immune cells. CVB3 mice exhibited a 1.8-fold ( $P < 0.0001$ ), 2.4-fold ( $P < 0.0001$ ), and 1.2-fold ( $P < 0.0001$ ) higher percentage of cardiac ASC-expressing, caspase-1-expressing, and IL-1 $\beta$ -expressing cells compared with uninfected controls

(Figure 2A–C), respectively. Along with this, a higher percentage of cardiac ASC-expressing DC (Figure 2D), ASC-expressing NK cells (Figure 2G) and ASC-expressing macrophages (Figure 2J) were detected in CVB3 mice compared with control animals. In parallel, the number of cardiac caspase-1-positive (Figure 2E,H,K) and IL-1 $\beta$ -positive (Figure 2F,I,L) DC, NK cells, and macrophages was also increased after CVB3 infection vs. corresponding controls. In contrast, CVB3 + colchicine mice showed lower numbers of cardiac ASC-expressing, caspase-1-expressing, and IL-1 $\beta$ -expressing DC, NK cells, and macrophages compared the CVB3 + PBS mice (Figure 2D–L). With respect to IL-1 $\beta$  at the protein level, no significant in-

**Figure 2** Colchicine reduces the presence of NLRP3 inflammasome-expressing cells in the left ventricle of experimental Coxsackievirus B3-induced myocarditis. Bar graphs represent the percentage of ASC-positive (A), caspase-1-positive (B), and IL-1 $\beta$ -positive (C) cells in the LV of control mice (white bars) or CVB3-infected mice (grey bars) treated with phosphate-buffered saline (PBS) (○) or 5  $\mu$ mol/kg BW colchicine (■). Furthermore, the amount of ASC-positive (D,G,J), caspase-1-positive (E,H,K), and IL-1 $\beta$ -positive (F,I,L) dendritic cells (CD11c<sup>+</sup>), natural killer cells (CD49<sup>+</sup>), and macrophages (F4/80<sup>+</sup>) in the different groups were assessed. Data are depicted as scatter plots with bars, showing individual data points and the mean  $\pm$  SEM. Statistical analysis was performed by using ordinary one-way ANOVA or Welch-ANOVA (\* $P$  < 0.05, \*\* $P$  < 0.01, \*\*\* $P$  < 0.001, and \*\*\*\* $P$  < 0.0001, with  $n$  = 4/group).



crease was observed in the LV homogenate, nor serum of CVB3 mice vs. control mice. Colchicine did not affect IL-1 $\beta$  protein levels in the LV (Figure S2A), whereas 1.1-fold ( $P < 0.05$ ) higher serum IL-1 $\beta$  levels were detected in CVB3 + colchicine vs. CVB3 + PBS mice (Figure S2B). Along with the observed increased NLRP3 activity in cardiac DC, NK cells and macrophages, the total percentage of DC, NK cells, and macrophages was elevated by 1.7-fold ( $P < 0.0001$ ), 2.1-fold ( $P < 0.0001$ ), and 2.0-fold ( $P < 0.0001$ ) in the myocardium of CVB3-infected mice, respectively (Figure S3A–C). These changes in percentages were also reflected in the number of events (Table S1), as shown by a 2.5-fold ( $P < 0.01$ ), 3.3-fold ( $P < 0.0001$ ), and 2.9-fold ( $P < 0.01$ ) higher event number of DC, NK cells, and macrophages, respectively, in CVB3 mice vs. controls. This increase was diminished by application of colchicine, as shown by the lower percentage and number of events of the respective cell population in CVB3 + colchicine vs. CVB3 + PBS mice.

### Colchicine abrogates splenic NLRP3 inflammasome activation in experimental Coxsackievirus B3-induced myocarditis

With the spleen being a reservoir of immune cells, which can be mobilized and subsequently migrate to the heart,<sup>26,27</sup> we next investigated the impact of colchicine on splenic inflammasome activation (Figure 3). In accordance with our own previous data,<sup>8</sup> the percentage of ASC- and IL-1 $\beta$ -expressing cells was elevated in the spleen of CVB3 mice compared with controls (Figure 3A + B). Oral application of colchicine vs. PBS treatment in CVB3-infected mice reduced the number of splenic ASC-positive and IL-1 $\beta$ -positive cells by 1.5-fold ( $P < 0.0001$ ) and 1.2-fold ( $P < 0.001$ ), respectively. Additionally, the amount of ASC-positive (Figure 3C,E,G) and IL-1 $\beta$ -positive (Figure 3D,F,H) DC, NK cells, and macrophages was higher in CVB3-infected mice compared with the respective controls. Colchicine abrogated this CVB3-induced effect, as indicated by a lower percentage of splenic ASC-expressing and IL-1 $\beta$ -expressing DC, NK cells, and macrophages in CVB3 + colchicine vs. CVB3 + PBS mice. In parallel, colchicine normalized the 4.1-fold ( $P < 0.05$ ) down-regulated splenic IL-1 $\beta$  protein levels observed in CVB3 mice to levels of control mice. (Figure S2C). Similar to the heart, the amount of splenic DC (Figure S4A), NK cells (Figure S4B), and macrophages (Figure S4C) was 1.3-fold ( $P < 0.0001$ ), 1.5-fold ( $P < 0.0001$ ), and 2.4-fold ( $P < 0.0001$ ) higher respectively in CVB3 compared with control mice. Further, the number of events of the respective cells were 1.2-fold (ns), 1.4-fold ( $P < 0.01$ ), and 2.0-fold ( $P < 0.01$ ) higher in CVB3 animals compared with control mice (Table S1). Application of colchicine lowered the percentage and number of events of all cell populations in CVB3 animals compared with PBS treatment (Figure S4 and Table S1).

### Colchicine alters left ventricular collagen composition in experimental Coxsackievirus B3-induced myocarditis

The CVB3-induced myocarditis is associated with cardiac fibrosis, as indicated by alterations in collagen I and III protein expression and reflected in an increased collagen I/III protein ratio.<sup>15</sup> In accordance, 3.9-fold ( $P < 0.01$ ), 4.1-fold ( $P < 0.01$ ), and 33.5-fold ( $P < 0.0001$ ) higher LV Col1a1, Col3a1, and LOX gene expression, respectively, was detected in CVB3-infected mice compared with uninfected controls (Figure S5). This was further associated with 4.4-fold ( $P < 0.01$ ) and 12-fold ( $P < 0.01$ ) higher LV collagen I protein expression in the total LV area (Figure 4A + B) and in the LV area, excluding all vessels and arteries of the analysis (Figure 4E), respectively when compared with uninfected controls. Protein expression of the compliant collagen III (Figure 4A,C,F) did not differ between controls and CVB3 mice. This was reflected in a 5.0-fold ( $P < 0.01$ ; Figure 4D) and 13-fold ( $P < 0.01$ ; Figure 4G) elevated LV collagen I/III protein ratio in the total LV area and in the LV area without vessels and arteries respectively of CVB3-infected mice vs. control animal. Colchicine intervention reduced LV Col1a1 and LOX mRNA expression (Figure S5A,C), and collagen I protein expression in the LV area excluding vessels and arteries (Figure 4E) in CVB3 + colchicine mice vs. CVB3 + PBS animals. The collagen I/III ratio was 2.2-fold ( $P < 0.05$ ; Figure 4D) and 2.9-fold ( $P < 0.05$ ; Figure 4G) lower in the total LV and in the LV area without vessels and arteries, respectively, in colchicine-treated CVB3 vs. CVB3 + PBS mice.

### Colchicine exerts anti-(fibro)inflammatory effects in cardiac cells

To finally investigate possible underlying mechanisms of the anti-(fibro)inflammatory potential of colchicine, *in vitro* infection experiments on FB and HL-1 cells were performed.

As shown in the Figure S6A–D, CVB3 infection of FB resulted in 1.3-fold ( $P < 0.05$ ), 1.5-fold ( $P < 0.01$ ), and 1.5-fold ( $P < 0.05$ ) higher gene expression of Col3a1,  $\alpha$ -SMA, and TGF- $\beta$ , respectively, compared with controls. Interestingly, only gene expression of Col3a1 was reduced by colchicine supplementation. Verification of these results at the protein level revealed changes of collagen deposition in FB after 24 and 72 h stimulation with colchicine (Figure 5A). Taking the cell number into account (Figure 5B), the resulting collagen amount per cell (Figure 5C) was increased in CVB3-infected FB vs. controls only after 72 h colchicine stimulation. Administration of colchicine to the media was able to reduce collagen levels in these cells.

Because inflammasome activation in cardiac resident cells is linked to cardiac fibrosis,<sup>28</sup> expression of NLRP3 compo-

**Figure 3** Colchicine abrogates splenic NLRP3 inflammasome activity in experimental Coxsackievirus B3-induced myocarditis. Bar graphs represent the percentage of total ASC-positive (A) and IL-1 $\beta$ -positive (B) cells in the spleen of control mice (white bars) or CVB3-infected mice (grey bars) treated with phosphate-buffered saline (PBS) (○) or 5  $\mu$ mol/kg BW colchicine (■). Similar to the investigations of the heart, the amount of ASC-expressing (C,E,G) and IL-1 $\beta$ -expressing (D,F,H) DC (CD11c<sup>+</sup>), NK cells (CD49<sup>+</sup>), and macrophages (F4/80<sup>+</sup>) in the spleen were determined. Data are depicted as scatter plots with bars, showing individual data points and the mean  $\pm$  SEM. Statistical analysis was performed by using ordinary one-way ANOVA or Welch-ANOVA (\* $P < 0.05$ , \*\* $P < 0.01$ , \*\*\* $P < 0.001$ , and \*\*\*\* $P < 0.0001$ , with  $n = 4$ /group).

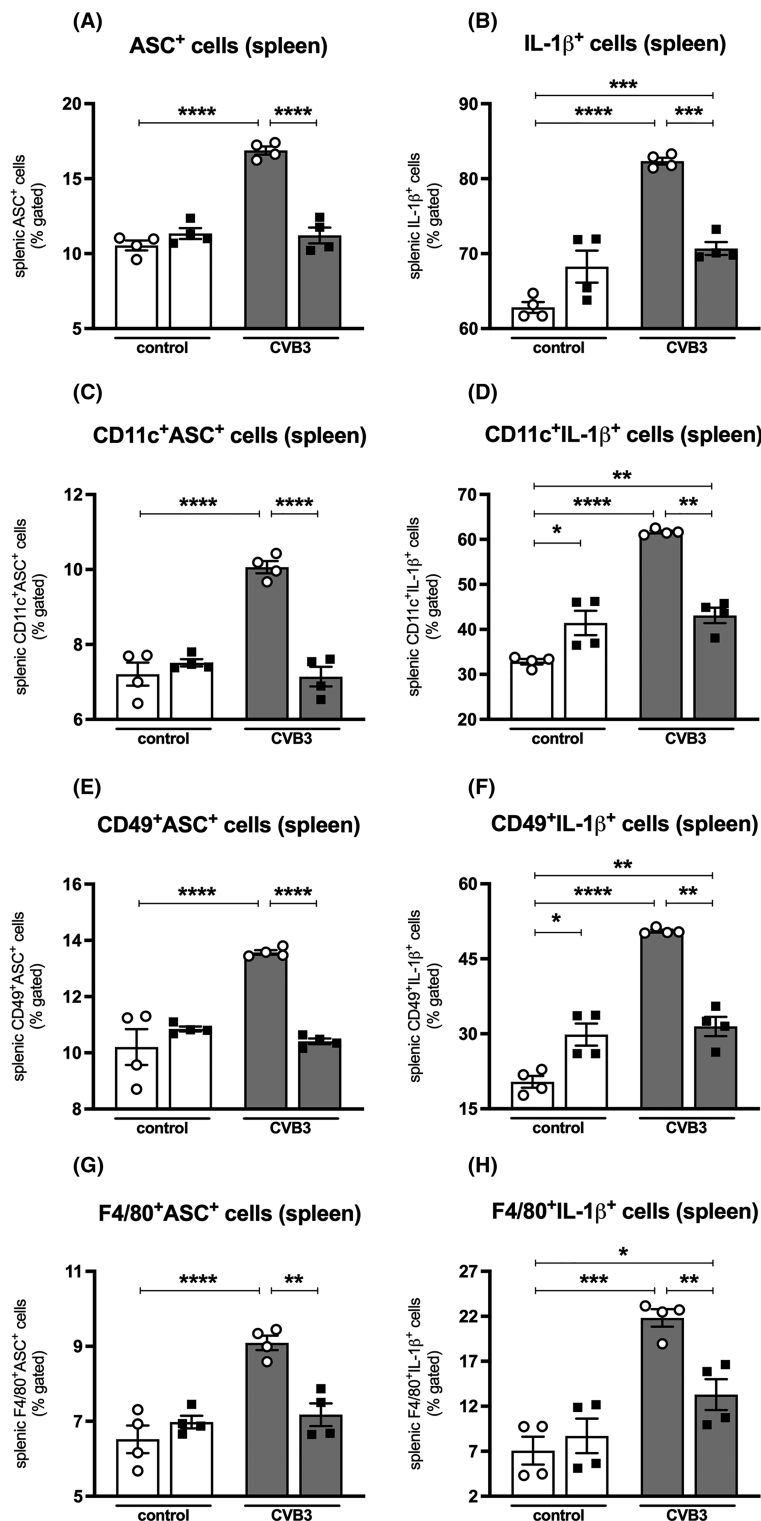
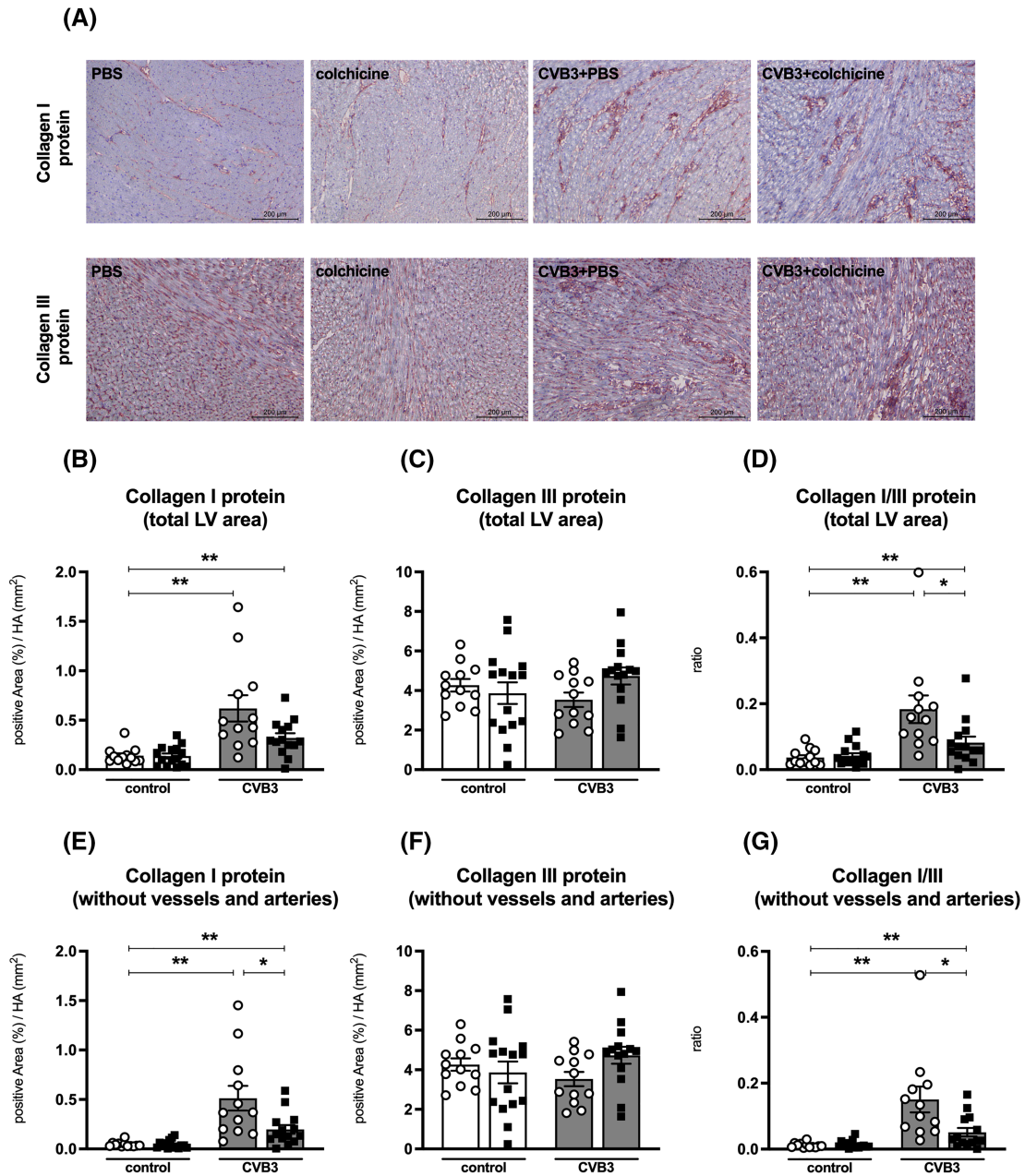


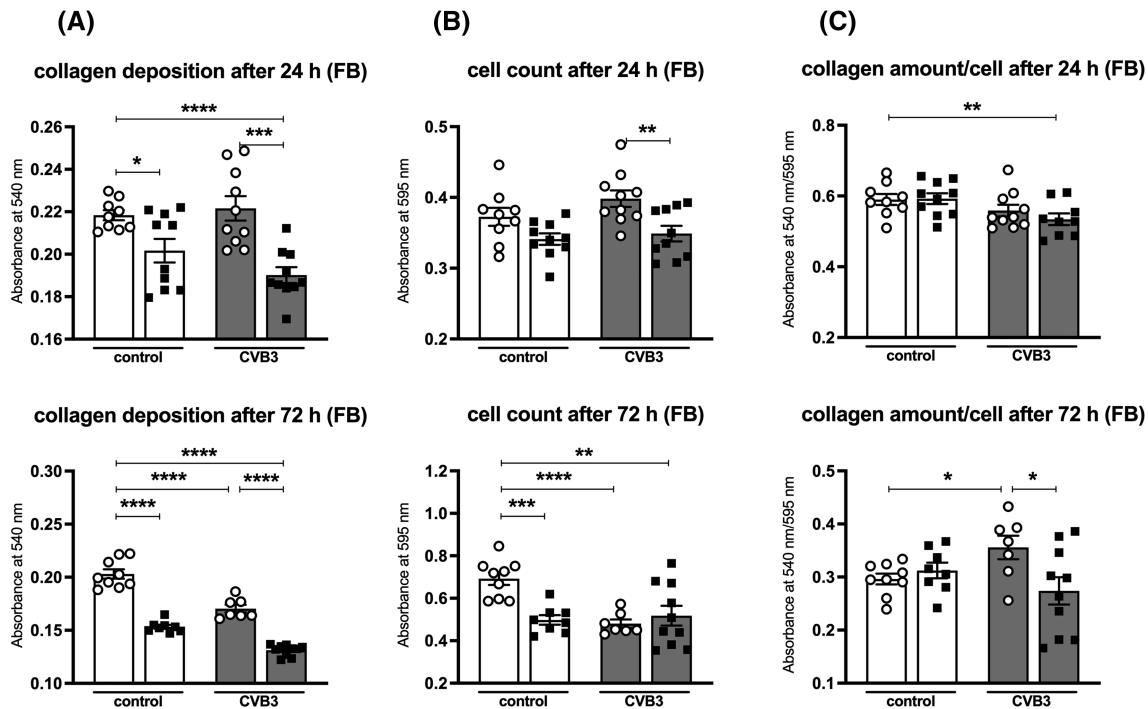
**Figure 4** Colchicine alters left ventricular collagen composition in experimental Coxsackievirus B3-induced myocarditis. To determine the impact of colchicine on cardiac fibrosis, LV cryosections were stained with antibodies directed against collagen I (A, upper row) and III (A, lower row). To illustrate changes in collagen expression, representative pictures (scale bar = 200  $\mu\text{m}$ ) of both stainings were depicted. Quantitative analysis of the stainings were performed via digital image analysis at a 100x magnification, and expressed as positive area (%) / heart area (HA;  $\text{mm}^2$ ). To distinguish between different types of fibrosis, LV samples were analysed including vessel and arteries (total LV area; B + C) and without vessels and arteries (interstitial fibrosis; E + F). Subsequently, the collagen I/III ratio of both analysis settings was calculated (D + G). Data of control mice (white bars) or CVB3-infected mice (grey bars) treated with phosphate-buffered saline (PBS) (o) or 5  $\mu\text{mol/kg}$  BW colchicine ( $\blacksquare$ ) were depicted as scatter plots with bars, showing individual data points and the mean  $\pm$  SEM. Statistical analysis was performed by using ordinary one-way ANOVA or Welch-ANOVA ( $*P < 0.05$ ,  $**P < 0.01$ ,  $***P < 0.001$ , and  $****P < 0.0001$ , with  $n = 12/\text{control} + \text{PBS}$ ,  $n = 15/\text{control} + \text{colchicine}$ ,  $n = 12/\text{CVB3} + \text{PBS}$ ,  $n = 14/\text{CVB3} + \text{colchicine}$ ).



ments in FB and HL-1 cells was measured (Figure 6). The percentage of ASC<sup>+</sup>, caspase-1<sup>+</sup>, and IL-1 $\beta$ <sup>+</sup> cells was 1.5-fold ( $P < 0.001$ ; Figure 6A), 1.4-fold ( $P < 0.01$ ; Figure 6B), and

1.9-fold ( $P < 0.001$ ; Figure 6C) higher in CVB3-infected FB compared with non-infected controls, respectively. Colchicine blunted NLRP3 inflammasome activation in CVB3-infected FB

**Figure 5** Colchicine decreases collagen deposition in Coxsackievirus B3-infected left ventricle-derived fibroblasts. To verify the impact of colchicine on the collagen protein level in CVB3-infected fibroblast (FB), a Sirius red (A) and crystal violet assay (B) were performed. For this purpose, FB were infected and subsequently stimulated for 24 h (upper row) and 72 h (lower row) with colchicine. Photometric analyses were performed at 540 and 595 nm for both the Sirius Red staining and crystal violet staining, using the Spectra Max 340PC microplate reader. In addition to the depicted absorbance values, collagen deposition was normalized against the cell number (collagen content/cell number; C). The scatter plots illustrate the individual data points and the mean  $\pm$  SEM of FB under control conditions (white bars) or in CVB3-infected cells (grey bars) treated without (○) or with 100 ng/mL colchicine (■). Statistical analysis was performed by using Welch-ANOVA (\* $P < 0.05$ , \*\* $P < 0.01$ , \*\*\* $P < 0.001$ , and \*\*\*\* $P < 0.0001$ , with  $n = 9$ –10/group for 24 h and  $n = 7$ –10/group for 72 h).



as illustrated by a 1.1-fold ( $P < 0.05$ ), 1.1-fold ( $P < 0.05$ ), and 1.2-fold ( $P < 0.01$ ) lower percentage of ASC<sup>+</sup> cells, caspase-1<sup>+</sup> cells, and IL-1 $\beta$ <sup>+</sup> cells vs. CVB3 FB, respectively. Infected HL-1 cells exhibited a 1.8-fold ( $P < 0.001$ ; Figure S7A), 1.4-fold ( $P < 0.001$ ; Figure S7B), and 3.2-fold ( $P < 0.01$ ; Figure S7C) higher percentage of ASC<sup>+</sup> cells, caspase-1<sup>+</sup> cells, and IL-1 $\beta$ <sup>+</sup> cells, respectively, compared with uninfected controls. Colchicine abrogated the CVB3-mediated increase in HL-1 cells expressing components of the NLRP3 inflammasome, as indicated by 1.3-fold ( $P < 0.01$ ), 1.2-fold ( $P < 0.001$ ), and 2.0-fold ( $P < 0.001$ ) lower numbers of ASC<sup>+</sup> cells, caspase-1<sup>+</sup> cells, and IL-1 $\beta$ <sup>+</sup> cells, compared with CVB3 HL-1 cells, respectively.

## Discussion

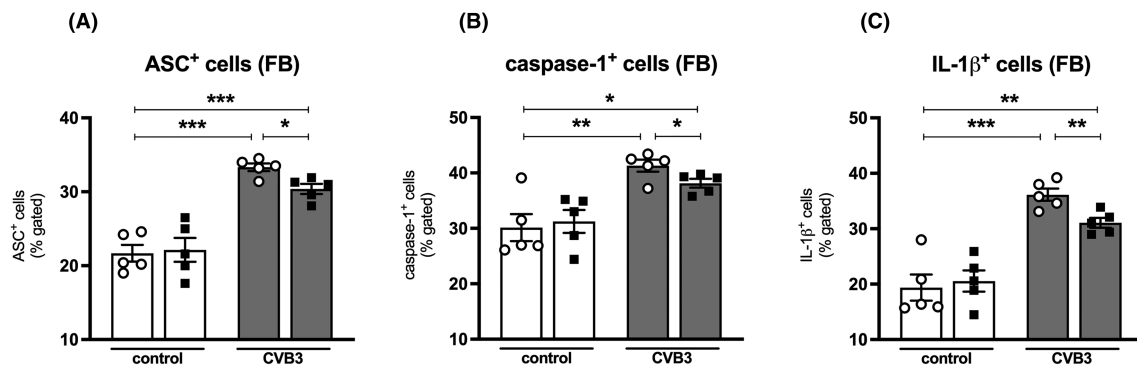
In the present study, we demonstrate that an intervention with colchicine during the acute phase of CVB3-induced myocarditis prevents deterioration of cardiac function. Colchicine exerts systemic immunomodulatory effects as indicated by a reduction in NLRP3 inflammasome activation and subsequent

IL-1 $\beta$  production in cardiac and splenic macrophages (F4/80<sup>+</sup> cells), NK cells (CD49b<sup>+</sup> cells), and DCs (CD11c<sup>+</sup> cells). Targeting the NLRP3 axis by colchicine did not exacerbate CVB3 load. *In vitro* experiments with murine LV-derived FB and HL-1 cardiomyocytes further showed that the colchicine-mediated reduction in NLRP3 inflammasome activation was extended to cardiac resident cells including fibroblasts and cardiomyocytes.

Due to direct viral toxicity and a consequent massive inflammatory response, viral persistence in myocarditis can be associated with an impaired prognosis.<sup>3</sup> For this clinical scenario, treatment options are not established since direct anti-viral drugs are not available for most cardiotropic viruses and global immunosuppressive interventions are contraindicated. The development of immunomodulatory strategies to increase viral clearance (e.g. via interferon- $\beta$ <sup>29</sup>) or to balance key pathways of an uncontrolled inflammatory response without compromising viral control as shown for eplerenone<sup>30</sup> would be important for advanced therapy options in viral myocarditis.<sup>31,32</sup>

As part of the inflammatory response in CVB3-induced myocarditis, a large number of immune cells including NK

**Figure 6** Colchicine reduces inflammasome activation in Coxsackievirus B3-infected left ventricle-derived fibroblasts. Expression of components of the NLRP3 inflammasome in primary cardiac fibroblast (FB) obtained via outgrowth culture was determined via flow cytometry. Graphs illustrate the percentage of ASC-positive (A), caspase-1-positive (B), and IL-1 $\beta$ -positive cells (C) under control conditions (white bars) or in CVB3-infected cells (grey bars) treated without (○) or with 100 ng/mL colchicine (■). Data are depicted as scatter plots with bars, showing individual data points and the mean  $\pm$  SEM. Statistical analysis was performed by using Welch-ANOVA ( $*P < 0.05$ ,  $**P < 0.01$ ,  $***P < 0.001$ , and  $****P < 0.0001$ , with  $n = 5$ /group).



cells, monocytes, and lymphocytes infiltrate into the inflamed areas of the heart.<sup>15</sup> The spleen is known to be a reservoir from which monocytes can migrate into the heart,<sup>26,27</sup> differentiate into macrophages and DCs, and mediate a detrimental immune reaction. CVB3-infected mice exhibit increased splenic and myocardial expression of NLRP3, ASC, and caspase-1 as well as a higher percentage of splenic ASC-expressing, caspase-1-expressing, and IL-1 $\beta$ -expressing DCs, NK cells, and macrophages compared with control mice.<sup>8</sup> Furthermore, cardiac infiltrating macrophages express high levels of NLRP3 and IL-1 $\beta$  in CVB3 mice and contribute to severe myocardial inflammation.<sup>33</sup> Similar to our own previous observations in MSC-treated CVB3 mice,<sup>8</sup> a lower number of splenic ASC-expressing, caspase-1-expressing, and IL-1 $\beta$ -expressing cells, indicative for a reduced NLRP3 inflammasome formation,<sup>34</sup> was present in colchicine-treated vs. PBS-treated CVB3 mice. Evaluation of cardiac inflammatory cells further indicated the presence of fewer cardiac ASC-expressing, caspase-1-expressing, and IL-1 $\beta$ -expressing DCs, NK cells, and macrophages, supporting the hypothesis that colchicine modulates the cardiosplenic axis, resulting in a diminished infiltration of NLRP3-active inflammatory cells into the heart. This systemic immunomodulatory effect of colchicine might explain the cardio-beneficial effects in colchicine-treated CVB3 mice, which is founded not solely on a reduction of NLRP3 inflammasome activation, but also of splenic and cardiac DCs, NK cells and macrophages. Our findings are therefore not contradictory *per se* to the increased myocardial and pancreatic damage and impaired cardiac function in CVB3-infected NLRP3 knockout mice compared with non-transgenic control mice, which might be due to the complete absence of NLRP3.<sup>35</sup> Interestingly, ubiquitous knock-down of the intracellular pattern recognition receptor NOD2 resulted in a reduced NLRP3 activation leading to an amelioration of experimental CVB3-induced myocarditis.<sup>9</sup> With the spleen being a target organ of CVB3,<sup>4</sup> it is conceivable that

partly splenectomised mice would exhibit a less pronounced infiltration of the heart with CVB3-infected immune cells, resulting in reduced cardiac inflammation and fibrosis, and improved LV function. However, resolution of cardiac inflammation upon CVB3 infection is a subtle balance of pro-inflammatory and anti-inflammatory immune responses, and splenectomy could also lead to increased severity. By the application of colchicine, we were able to modulate this cardiosplenic axis, as indicated by a reduced infiltration of potentially CVB3-infected immune cells into the heart, which can be explained by the decreased cardiac CVB3 copy number and lower percentage of ASC-expressing, caspase-1-expressing, and IL-1 $\beta$ -expressing cells in the colchicine-treated CVB3 mice. In contrast to our study, Smilde *et al.*<sup>36</sup> showed that i.p. injected colchicine led to higher cardiac CVB3 mRNA levels and aggravated CVB3-induced myocarditis in CH3 mice, leading to severe illness and mortality on the third day after infection.<sup>36</sup> However, this might be due to the chosen administered dose and application route,<sup>37</sup> because increased inflammatory cell numbers (lymphocytes, neutrophils, and macrophages) were observed in the pancreas and heart of colchicine-treated vs. untreated control mice, indicative for well-known drug-induced toxicity.<sup>38</sup> Compared with Smilde *et al.*,<sup>36</sup> we administered the same dose of colchicine, which also has been successfully used in several other experimental scenarios,<sup>39,40</sup> but per oral gavage. Furthermore, differences in the outcome of the studies due to the use of different mouse strains, resulting in a different sensitivity to colchicine-induced toxicity, is also a possible explanation for the observed differences between the studies.

In parallel to the reduced cardiac infiltrating immune cells and conforming with the anti-fibrotic effects of colchicine,<sup>12</sup> LV interstitial fibrosis was reduced in colchicine-treated vs. PBS-injected CVB3 animals. Subsequent analyses on LV-derived FB further supported the hypothesis that CVB3-mediated inflammasome activation in cardiac resident

cells is directly linked to myofibroblast activation and subsequent tissue fibrosis, as shown for myocardial ischaemia/reperfusion injury,<sup>41</sup> for angiotensin II-induced heart failure,<sup>42</sup> and for cancer.<sup>43</sup> In addition to alterations of the collagen I/III protein ratio, we demonstrated improved systolic and diastolic function in CVB3 + colchicine vs. CVB3 mice. This is in accordance with the observed improvement in left ventricular remodelling and cardiac function seen following colchicine treatment in experimental acute myocardial infarction.<sup>44</sup> The improvement of cardiac function upon colchicine administration, cannot be explained by the anti-fibrotic effects of colchicine alone, but also by its anti-apoptotic effects. It is well-known that CVB3 infection has a direct cytotoxic effect on cardiomyocytes, which is also triggered by oxidative stress.<sup>17</sup> In agreement with our own previous findings,<sup>17,18,25</sup> increased oxidative stress and apoptosis as well as serum cTN-I levels<sup>18</sup> were detected in CVB3 mice. Treatment with colchicine reduced both oxidative stress and apoptosis and was finally translated in the reduction in CVB3 copy number and lower cTN-I levels in the serum of the CVB3 + colchicine mice.

Taken together, to our knowledge, this study is the first investigating the impact of colchicine on disease progression involving modulation of the cardiosplenic axis. We show that colchicine applied in the early phase of viral infection decreases splenic NLRP3 inflammasome activity, which was associated with lower myocardial immune cell infiltration and improved LV function. Additionally to these effects on the cardiosplenic axis, *in vitro* experiments further illustrated that colchicine inhibits NLRP3 inflammasome activation in FB and HL-1 cardiomyocytes, blunting their (fibro)inflammatory potential. Importantly, no exacerbation of CVB3 was detected, showing that colchicine did not negatively influence the viral defence reaction of the host, therefore allowing application of colchicine during viral persistence. These results, together with the findings that SARS-CoV-2-infected macrophages, can migrate into the heart,<sup>45</sup> and SARS-CoV2 leads to NLRP3 activation<sup>46,47</sup> further supporting the hypothesis of DeFtereos *et al.*<sup>48</sup> that colchicine may also be useful to treat COVID-19-associated heart diseases. Based on the positive immunomodulatory effects, colchicine provides a new potential treatment option for acute viral myocarditis. However, the safety and efficacy of colchicine in myocarditis need to be investigated under a clinical study setting. Here, a properly designed clinical study should include follow-up re-biopsy to allow quantification of myocardial inflammation and viral activity.

## Acknowledgements

The authors would like to acknowledge the assistance of the BCRT Flow Cytometry Lab and Annika Koschel, Kerstin Puhl,

and Marzena Sosnowski (in alphabetical order) for their excellent technical support. In addition, we like to thank Nicola Brindle for scientific language check and editing. Open Access funding enabled and organized by Projekt DEAL.

## Conflict of interest

C. T. has received speaker fees and/or contributions to congresses from Abbott, Abiomed, Astra Zeneca, Bayer, Berlin Chemie, Novartis, Pfizer, and Servier; all outside the submitted work.

## Funding

This work was supported by the Friede Springer Heart Foundation to S.V.L.

## Supporting information

Additional supporting information may be found online in the Supporting Information section at the end of the article.

**Figure S1.** Colchicine reduces apoptosis and oxidative stress in experimental Coxsackievirus B3-induced myocarditis. Indicative for cardiomyocyte apoptosis, B-cell lymphoma 2 (Bcl-2; A) and Bcl-2-associated X protein (Bax; B) gene expression was analysed and the Bcl-2/Bax ratio (C) was calculated in control mice (white bars) or CVB3-infected mice (grey bars) treated with PBS (○) or 5 μmol/kg BW colchicine (■). Additionally, gene expression of NADPH oxidase (NOX) 1 (D), NOX4 (E), and superoxide dismutase (SOD) 2 (F), as markers for oxidative stress, were measured via real-time PCR. All data are depicted as scatter plots with bars, showing individual data points and the mean±SEM. Statistical analysis was performed by using ordinary one-way ANOVA or Welch-ANOVA (\*p<0.05, \*\*p<0.01, \*\*\*p<0.001, and \*\*\*\*p<0.0001; with n=11-12/control + PBS, n=11-15/control + colchicine, n=11-12/CVB3 + PBS, n=12-13/CVB3 + colchicine).

**Figure S2.** Colchicine modulates organ-specific and systemic interleukin-1β expression in experimental Coxsackievirus B3-induced myocarditis. To further investigate the impact of colchicine on interleukin (IL)-1β expression, an IL-1β ELISA on LV homogenates (A), serum (B), and spleen homogenates (C) was performed. Graphs show the amount of IL-1β protein in the respective organ (ng/250 μg protein) or serum (ng/mL) of control mice (white bars) or CVB3-infected mice (grey bars) treated with PBS (○) or 5 μmol/kg BW colchicine (■). Data are depicted as scatter plots with bars, showing individual data points and the mean±SEM. Statistical analysis was performed

by using ordinary one-way ANOVA or Welch-ANOVA (\* $p < 0.05$ , and \*\*\* $p < 0.001$ ; with  $n = 5-6$ /group for A + C and  $n = 7$ /control + PBS,  $n = 12$ /control + colchicine,  $n = 16$ /CVB3 + PBS,  $n = 9$ /CVB3 + colchicine for B).

**Figure S3.** Colchicine reduces cardiac immune cell presence in experimental Coxsackievirus B3-induced myocarditis. Bar graphs represent the percentage of dendritic cells (DC; CD11c<sup>+</sup> cells; A), natural killer (NK) cells (CD49<sup>+</sup> cells; B) and macrophages (F4/80<sup>+</sup> cells; C) in the heart of control mice (white bars) or CVB3-infected mice (grey bars) treated with PBS (○) or 5 μmol/kg BW colchicine (■). Data are depicted as scatter plots with bars, showing individual data points and the mean ± SEM. Statistical analysis was performed by using ordinary one-way ANOVA or Welch-ANOVA (\* $p < 0.05$ , \*\* $p < 0.01$ , \*\*\* $p < 0.001$ , and \*\*\*\* $p < 0.0001$ , with  $n = 4$ /group).

**Figure S4.** Colchicine diminishes the number of splenic dendritic cells, natural killer cells, and macrophages in experimental Coxsackievirus B3-induced myocarditis. Bar graphs represent the percentage of DC (A), NK (B), and macrophages (C) in the spleen of control mice (white bars) or CVB3-infected mice (grey bars) treated with PBS (○) or 5 μmol/kg BW colchicine (■). Data are depicted as scatter plots with bars, showing individual data points and the mean ± SEM. Statistical analysis was performed by using ordinary one-way ANOVA or Welch-ANOVA (\* $p < 0.05$ , \*\* $p < 0.01$ , \*\*\* $p < 0.001$ , and \*\*\*\* $p < 0.0001$ , with  $n = 4$ /group).

**Figure S5.** Colchicine alters left ventricular gene expression of pro-fibrotic factors in experimental Coxsackievirus B3-induced myocarditis. To determine the impact of colchicine on cardiac fibrosis, gene expression of LV Col1a1 (A), Col3a1 (B), and lysyloxidase (LOX; C) was investigated by real-time PCR. Bar graphs depict gene expression level of the respective target genes in the LV of control mice (white bars) or CVB3-infected mice (grey bars) treated with PBS (○) or 5 μmol/kg BW colchicine (■). Data are depicted as scatter plots with bars, showing individual data points and the mean ± SEM. Statistical analysis was performed by using ordinary one-way ANOVA or Welch-ANOVA (\* $p < 0.05$ , \*\* $p < 0.01$ , \*\*\* $p < 0.001$ , and \*\*\*\* $p < 0.0001$ , with  $n = 12$ /control + PBS,  $n = 15$ /control + colchicine,  $n = 12$ /CVB3 + PBS,  $n = 14$ /CVB3 + colchicine).

**Figure S6.** Colchicine modulates left ventricular gene expression of pro-fibrotic factors in Coxsackievirus B3-infected left ventricle-derived fibroblasts. Similar to the investigations on LV tissue, the impact of colchicine on the expression of markers for fibrosis in FB was investigated via real-time PCR. As target genes, mRNA levels of Col1a1 (A), Col3a1 (B), α-smooth muscle actin (α-SMA; C) and transforming growth factor-β (TGF-β; D) were analysed. The scatter plots illustrate the individual data points and the mean ± SEM of FB under control conditions (white bars) or in CVB3-infected cells (grey bars) treated without (○) or with 100 ng/mL colchicine (■). Statistical analysis was performed by using Welch-ANOVA (\* $p < 0.05$ , \*\* $p < 0.01$ , \*\*\* $p < 0.001$ , and \*\*\*\* $p < 0.0001$ , with  $n = 5$ /group).

**Figure S7.** Colchicine reduces inflammasome activation in Coxsackievirus B3-infected cardiomyocytes. Expression of components of the NLRP3 inflammasome was determined in the cardiomyocyte cell line HL-1 via flow cytometry. Graphs illustrate the percentage of ASC- (A), caspase-1- (B), and IL-1β-positive cells (C) under control conditions (white bars) or in CVB3-infected cells (grey bars) treated without (○) or with 100 ng/mL colchicine (■). Data are depicted as scatter plots with bars, showing individual data points and the mean ± SEM. Statistical analysis was performed by using Welch-ANOVA (\* $p < 0.05$ , \*\* $p < 0.01$ , \*\*\* $p < 0.001$ , and \*\*\*\* $p < 0.0001$ , with  $n = 6$ /group).

**Table S1.** Colchicine diminishes the cell counts of dendritic cells, natural killer cells, and macrophages in experimental Coxsackievirus B3-induced myocarditis. The table illustrates the number of events (cell count) measured via flow cytometry of dendritic cells (DC; CD11c + cells); natural killer (NK) cells (CD49 + cells), and macrophages (F4/80 + cells) in the heart and spleen of control mice and CVB3-infected mice treated with PBS or 5 μmol/kg BW colchicine. To analyse the respective cell population,  $1 \times 10^6$  splenocytes or  $0.9-1.2 \times 10^6$  cardiac MNCs were stained with anti-CD11c, anti-CD49, and anti-F4/80 antibodies. Data are presented as mean ± SEM. Statistical analysis was performed by using ordinary one-way ANOVA or Welch-ANOVA (\* $p < 0.05$ , \*\* $p < 0.01$ , \*\*\* $p < 0.001$ , and \*\*\*\* $p < 0.0001$  versus control mice; # $p < 0.05$ , ## $p < 0.01$ , ### $p < 0.001$ , and #### $p < 0.0001$  versus CVB3 mice, with  $n = 4$ /group).

## References

1. Tschope C, Cooper LT, Torre-Amione G, Van Linthout S. Management of myocarditis-related cardiomyopathy in adults. *Circ Res* 2019; **124**: 1568–1583.
2. Van Linthout S, Klingel K, Tschope C. SARS-CoV-2-related myocarditis-like syndromes Shakespeare's question: what's in a name? *Eur J Heart Fail* 2020; **22**: 922–925.
3. Tschope C, Ammirati E, Bozkurt B, Caforio ALP, Cooper LT, Felix SB, Hare JM, Heidecker B, Heymans S, Hübner N, Kelle S, Klingel K, Maatz H, Parwani AS, Spillmann F, Starling RC, Tsutsui H, Seferovic P, Van Linthout S. Myocarditis and inflammatory cardiomyopathy: current evidence and future directions. *Nat Rev Cardiol* 2021; **18**: 169–193.
4. Klingel K, Stephan S, Sauter M, Zell R, McManus BM, Bultmann B, Kandolf R. Pathogenesis of murine enterovirus

- myocarditis: virus dissemination and immune cell targets. *J Virol* 1996; **70**: 8888–8895.
5. Leuschner F, Courties G, Dutta P, Mortensen LJ, Gorbатов R, Sena B, Novobrantseva TI, Borodovsky A, Fitzgerald K, Koteliansky V, Iwamoto Y, Bohlender M, Meyer S, Lasitschka F, Meder B, Katus HA, Lin C, Libby P, Swirski FK, Anderson DG, Weissleder R, Nahrendorf M. Silencing of CCR2 in myocarditis. *Eur Heart J* 2015; **36**: 1478–1488.
  6. Latz E, Xiao TS, Stutz A. Activation and regulation of the inflammasomes. *Nat Rev Immunol* 2013; **13**: 397–411.
  7. Toldo S, Kannan H, Bussani R, Anzini M, Sonnino C, Sinagra G, Merlo M, Mezzaroma E, De-Giorgio F, Silvestri F, van Tassel BW, Baldi A, Abbate A. Formation of the inflammasome in acute myocarditis. *Int J Cardiol* 2014; **171**: e119–e121.
  8. Miteva K, Pappritz K, Sosnowski M, el-Shafeey M, Müller I, Dong F, Savvatis K, Ringe J, Tschöpe C, van Linthout S. Mesenchymal stromal cells inhibit NLRP3 inflammasome activation in a model of coxsackievirus B3-induced inflammatory cardiomyopathy. *Sci Rep* 2018; **8**: 2820.
  9. Tschöpe C, Müller I, Xia Y, Savvatis K, Pappritz K, Pinkert S, Lassner D, Heimesaat MM, Spillmann F, Miteva K, Bereswill S, Schultheiss HP, Fechner H, Pieske B, Kühl U, van Linthout S. NOD2 (nucleotide-binding oligomerization domain 2) is a major pathogenic mediator of coxsackievirus B3-induced myocarditis. *Circ Heart Fail* 2017; **10**: e003870.
  10. Nuki G. Colchicine: its mechanism of action and efficacy in crystal-induced inflammation. *Curr Rheumatol Rep* 2008; **10**: 218–227.
  11. Chaldakov GN. Colchicine, a microtubule-disassembling drug, in the therapy of cardiovascular diseases. *Cell Biol Int* 2018; **42**: 1079–1084.
  12. Akodad M, Fauconnier J, Sicard P, Huet F, Blandel F, Bourret A, de Santa Barbara P, Aguilhon S, LeGall M, Hugon G, Lacampagne A, Roubille F. Interest of colchicine in the treatment of acute myocardial infarct responsible for heart failure in a mouse model. *Int J Cardiol* 2017; **240**: 347–353.
  13. Cosyns B, Plein S, Nihoyanopoulos P, Smiseth O, Achenbach S, Andrade MJ, Pepi M, Ristic A, Imazio M, Paelinck B, Lancellotti P, European Association of Cardiovascular Imaging (EACVI), European Society of Cardiology Working Group (ESC WG) on Myocardial and Pericardial diseases. European Association of Cardiovascular Imaging (EACVI) position paper: multimodality imaging in pericardial disease. *Eur Heart J Cardiovasc Imaging* 2015; **16**: 12–31.
  14. Adler Y, Charron P, Imazio M, Badano L, Barón-Esquivias G, Bogaert J, Brucato A, Gueret P, Klingel K, Lionis C, Maisch B, Mayosi B, Pavie A, Ristic AD, Sabaté Tenas M, Seferovic P, Swedberg K, Tomkowski W, ESC Scientific Document Group. 2015 ESC guidelines for the diagnosis and management of pericardial diseases: the task force for the diagnosis and Management of Pericardial Diseases of the European Society of Cardiology (ESC) endorsed by: the European Association for Cardio-Thoracic Surgery (EACTS). *Eur Heart J* 2015; **36**: 2921–2964.
  15. Pappritz K, Savvatis K, Miteva K, Kerim B, Dong F, Fechner H, Müller I, Brandt C, Lope B, González A, Ravassa S, Klingel K, Diez J, Reinke P, Volk HD, van Linthout S, Tschöpe C. Immunomodulation by adoptive regulatory T-cell transfer improves coxsackievirus B3-induced myocarditis. *FASEB J* 2018; fj201701408R.
  16. Pappritz K, Savvatis K, Koschel A, Miteva K, Tschöpe C, Van Linthout S. Cardiac (myo)fibroblasts modulate the migration of monocyte subsets. *Sci Rep* 2018; **8**: 5575.
  17. Van Linthout S, Savvatis K, Miteva K, Peng J, Ringe J, Warstat K, Schmidt-Lucke C, Sittinger M, Schultheiss HP, Tschöpe C. Mesenchymal stem cells improve murine acute coxsackievirus B3-induced myocarditis. *Eur Heart J* 2011; **32**: 2168–2178.
  18. Miteva K, Haag M, Peng J, Savvatis K, Becher PM, Seifert M, Warstat K, Westermann D, Ringe J, Sittinger M, Schultheiss HP, Tschöpe C, van Linthout S. Human cardiac-derived adherent proliferating cells reduce murine acute coxsackievirus B3-induced myocarditis. *PLoS ONE* 2011; **6**: e28513.
  19. Miteva K, Pappritz K, El-Shafeey M, Dong F, Ringe J, Tschöpe C, van Linthout S. Mesenchymal stromal cells modulate monocytes trafficking in coxsackievirus B3-induced myocarditis. *Stem Cells Transl Med* 2017; **6**: 1249–1261.
  20. Spillmann F, Miteva K, Pieske B, Tschöpe C, van Linthout S. High-density lipoproteins reduce endothelial-to-mesenchymal transition. *Arterioscler Thromb Vasc Biol* 2015; **35**: 1774–1777.
  21. Van Linthout S, Elsanhoury A, Klein O, Sosnowski M, Miteva K, Lassner D, Abou-el-Enein M, Pieske B, Kühl U, Tschöpe C. Telbivudine in chronic lymphocytic myocarditis and human parvovirus B19 transcriptional activity. *ESC Heart Fail* 2018; **5**: 818–829.
  22. Spillmann F, Graiani G, Van Linthout S, Meloni M, Campesi I, Lagrasta C, Westermann D, Tschöpe C, Quaini F, Emanuelli C, Madeddu P. Regional and global protective effects of tissue kallikrein gene delivery to the peri-infarct myocardium. *Regen Med* 2006; **1**: 235–254.
  23. Van Linthout S, Spillmann F, Riad A, Trimpert C, Lievens J, Meloni M, Escher F, Filenberg E, Demir O, Li J, Shakibaei M, Schimke I, Staudt A, Felix SB, Schultheiss HP, de Geest B, Tschöpe C. Human apolipoprotein A-I gene transfer reduces the development of experimental diabetic cardiomyopathy. *Circulation* 2008; **117**: 1563–1573.
  24. Müller I, Pappritz K, Savvatis K, Puhl K, Dong F, El-Shafeey M, Hamdani N, Hamann I, Noutsias M, Infante-Duarte C, Linke WA, van Linthout S, Tschöpe C. CX3CR1 knockout aggravates coxsackievirus B3-induced myocarditis. *PLoS ONE* 2017; **12**: e0182643.
  25. Müller I, Vogl T, Pappritz K, Miteva K, Savvatis K, Rohde D, Most P, Lassner D, Pieske B, Kühl U, van Linthout S, Tschöpe C. Pathogenic role of the damage-associated molecular patterns S100A8 and S100A9 in coxsackievirus B3-induced myocarditis. *Circ Heart Fail* 2017; **10**: e004125.
  26. Ismahil MA, Hamid T, Bansal SS, Patel B, Kingery JR, Prabhu SD. Remodeling of the mononuclear phagocyte network underlies chronic inflammation and disease progression in heart failure: critical importance of the cardiopulmonary axis. *Circ Res* 2014; **114**: 266–282.
  27. Swirski FK, Nahrendorf M, Eitzrodt M, Wildgruber M, Cortez-Retamozo V, Panizzi P, Figueiredo JL, Kohler RH, Chudnovskiy A, Waterman P, Aikawa E, Mempel TR, Libby P, Weissleder R, Pittet MJ. Identification of splenic reservoir monocytes and their deployment to inflammatory sites. *Science* 2009; **325**: 612–616.
  28. Zhang X, Qu H, Yang T, Kong X, Zhou H. Regulation and functions of NLRP3 inflammasome in cardiac fibrosis: current knowledge and clinical significance. *Biomed Pharmacother* 2021; **143**: 112219.
  29. Kühl U, Pauschinger M, Schwimmbeck PL, Seeberg B, Lober C, Noutsias M, Poller W, Schultheiss HP. Interferon-beta treatment eliminates cardiotoxic viruses and improves left ventricular function in patients with myocardial persistence of viral genomes and left ventricular dysfunction. *Circulation* 2003; **107**: 2793–2798.
  30. Tschöpe C, Van Linthout S, Jäger S, Arndt R, Trippel T, Müller I, Elsanhoury A, Rutschow S, Anker SD, Schultheiss HP, Pauschinger M, Spillmann F, Pappritz K. Modulation of the acute defence reaction by eplerenone prevents cardiac disease progression in viral myocarditis. *ESC Heart Fail* 2020; **7**: 2838–2852.
  31. Van Linthout S, Tschöpe C. The quest for anti-inflammatory and immunomodulatory strategies in heart failure. *Clin Pharmacol Ther* 2019; **106**: 1198–1208.
  32. Elsanhoury A, Tschöpe C, Van Linthout S. A toolbox of potential immune-related therapies for inflammatory cardiomyopathy. *J Cardiovasc Transl Res* 2020; **14**: 75–87.
  33. Bao J, Sun T, Yue Y, Xiong S. Macrophage NLRP3 inflammasome activated by CVB3 capsid proteins contributes to

- the development of viral myocarditis. *Mol Immunol* 2019; **114**: 41–48.
34. Wang Y, Gao B, Xiong S. Involvement of NLRP3 inflammasome in CVB3-induced viral myocarditis. *Am J Physiol Heart Circ Physiol* 2014; **307**: H1438–H1447.
  35. Wang C, Fung G, Deng H, Jagdeo J, Mohamud Y, Xue YC, Jan E, Hirota JA, Luo H. NLRP3 deficiency exacerbates enterovirus infection in mice. *FASEB J* 2019; **33**: 942–952.
  36. Smilde BJ, Woudstra L, Fong Hing G, Wouters D, Zeerleder S, Murk JL, van Ham M, Heymans S, Juffermans LJM, van Rossum AC, Niessen HWM, Krijnen PAJ, Emmens RW. Colchicine aggravates coxsackievirus B3 infection in mice. *Int J Cardiol* 2016; **216**: 58–65.
  37. Maestroni S, Imazio M, Valenti A, Assolari A, Brucato A. Is colchicine really harmful in viral myocarditis? *Int J Cardiol* 2017; **229**: 42.
  38. Milner CM, Higman VA, Day AJ. TSG-6: a pluripotent inflammatory mediator? *Biochem Soc Trans* 2006; **34**: 446–450.
  39. Craig DH, Owen CR, Conway WC, Walsh MF, Downey C, Basson MD. Colchicine inhibits pressure-induced tumor cell implantation within surgical wounds and enhances tumor-free survival in mice. *J Clin Invest* 2008; **118**: 3170–3180.
  40. Feng G, Kaplowitz N. Colchicine protects mice from the lethal effect of an agonistic anti-Fas antibody. *J Clin Invest* 2000; **105**: 329–339.
  41. Kawaguchi M, Takahashi M, Hata T, Kashima Y, Usui F, Morimoto H, Izawa A, Takahashi Y, Masumoto J, Koyama J, Hongo M, Noda T, Nakayama J, Sagara J, Taniguchi S, Ikeda U. Inflammasome activation of cardiac fibroblasts is essential for myocardial ischemia/reperfusion injury. *Circulation* 2011; **123**: 594–604.
  42. Bracey NA, Gershkovich B, Chun J, Vilaysane A, Meijndert HC, Wright JR Jr, Fedak PW, Beck PL, Muruve DA, Duff HJ. Mitochondrial NLRP3 protein induces reactive oxygen species to promote Smad protein signaling and fibrosis independent from the inflammasome. *J Biol Chem* 2014; **289**: 19571–19584.
  43. Ershaid N, Sharon Y, Doron H, Raz Y, Shani O, Cohen N, Monteran L, Leider-Trejo L, Ben-Shmuel A, Yassin M, Gerlic M, Ben-Baruch A, Pasmanik-Chor M, Apte R, Erez N. NLRP3 inflammasome in fibroblasts links tissue damage with inflammation in breast cancer progression and metastasis. *Nat Commun* 2019; **10**: 4375.
  44. Fujisue K, Sugamura K, Kurokawa H, Matsubara J, Ishii M, Izumiya Y, Kaikita K, Sugiyama S. Colchicine improves survival, left ventricular remodeling, and chronic cardiac function after acute myocardial infarction. *Circ J* 2017; **81**: 1174–1182.
  45. Tavazzi G, Pellegrini C, Maurelli M, Belliato M, Sciutti F, Bottazzi A, Sepe PA, Resasco T, Camporotondo R, Bruno R, Baldanti F, Paolucci S, Pelenghi S, Iotti GA, Mojoli F, Arbustini E. Myocardial localization of coronavirus in COVID-19 cardiogenic shock. *Eur J Heart Fail* 2020; **22**: 911–915.
  46. Shi CS, Nabar NR, Huang NN, Kehrl JH. SARS-coronavirus open reading frame-8b triggers intracellular stress pathways and activates NLRP3 inflammasomes. *Cell Death Dis* 2019; **5**: 101.
  47. Siu KL, Yuen KS, Castano-Rodriguez C, Ye ZW, Yeung ML, Fung SY, Yuan S, Chan CP, Yuen KY, Enjuanes L, Jin DY. Severe acute respiratory syndrome coronavirus ORF3a protein activates the NLRP3 inflammasome by promoting TRAF3-dependent ubiquitination of ASC. *FASEB J* 2019; **33**: 8865–8877.
  48. Devereos SG, Giannopoulos G, Vrachatis DA, Siasos GD, Giotaki SG, Gargalianos P, Metallidis S, Sianos G, Baltagiannis S, Panagopoulos P, Dolianitis K, Randou E, Syrigos K, Kotanidou A, Koulouris NG, Milionis H, Sipsas N, Gogos C, Tsoukalas G, Olympios CD, Tsagalou E, Migdalis I, Gerakari S, Angelidis C, Alexopoulos D, Davlouros P, Hahalis G, Kanonidis I, Katritsis D, Kolettis T, Manolis AS, Michalis L, Naka KK, Pyrgakis VN, Toutouzas KP, Triposkiadis F, Tsioufis K, Vavouranakis E, Martinèz-Dolz L, Reimers B, Stefanini GG, Cleman M, Goudevenos J, Tsiodras S, Tousoulis D, Iliodromitis E, Mehran R, Dangas G, Stefanadis C, GRECCO-19 investigators. Effect of colchicine vs standard care on cardiac and inflammatory biomarkers and clinical outcomes in patients hospitalized with coronavirus disease 2019: the GRECCO-19 randomized clinical trial. *JAMA Netw Open* 2020; **3**: e2013136.